Existence of fcc-Packed Spherical Micelles in Diblock Copolymer Melt

Yen-Yu Huang,[†] Jen-Yung Hsu,[†] Hsin-Lung Chen,*[,†] and Takeji Hashimoto*[,‡]

Department of Chemical Engineering, National Tsing Hua University, Hsin-Chu 30013, Taiwan, Advanced Science Research Center, Japan Atomic Energy Agency, Naka-gun, Ibaraki Prefecture 319-1195, Japan

Received September 16, 2006
Revised Manuscript Received December 27, 2006

Crystallization is a self-ordering process that prevails among various systems ranging from microscopic objects such as atoms and molecules to mesoscopic colloidal particles. Above certain threshold concentrations, colloidal particles with uniform size can crystallize into different lattice structures governed by their geometric shape and interaction potential.[1] Body-centered cubic (bcc) and closely packed lattices (either face-centered cubic (fcc) or hexagonally close-packed (hcp)) are the common structures formed by spherical colloids. Steep interaction potentials normally favor the close packing, whereas bcc is the more stable symmetry under softer interactions.[2,3]

Micelles formed by block copolymers in the melt and the solution are soft colloids that also exhibit the propensity to crystallize under appropriate conditions.[4,5] In contrast to hard spherical colloids, the spherical micelles formed by neat diblock copolymers in the quiescent melt have never been found to organize in closely packed lattices apart from bcc packing. However, self-consistent mean-field (SCMF) calculations have predicted a closely packed sphere (CPS) phase situating in a very narrow temperature window between bcc phase and a disordered homogeneous phase.[6,7] The reason why such a CPS phase was difficult to access experimentally may be due to the strong thermal fluctuations that disrupt the long-range order of the CPS phase into a disordered micelle phase at elevated temperatures.[8,9] The absence of CPS phase has also been attributed its instability relative to the disordered micelle phase in a recent theoretical study, where the disordered state was considered to consist of disordered spherical micelles instead of being a homogeneous melt with only thermal concentration fluctuations.[10] In this case, CPS phase was shown to be thermodynamically unstable because the gain in translational entropy allowed the disordered micelle regime to supersede the CPS phase.[10]

Herein we present the experimental observation of the close packing in the form of an fcc lattice of the spherical micelles formed by an asymmetric diblock copolymer in the quiescent melt. We will show that this fcc phase developed in a narrow temperature region upon cooling from the disordered micelle phase.

The system under study was a poly(ethylene oxide)-*block*-poly(1,4-butadiene) (PEO-*b*-PB) with the number-average molecular weights of PEO and PB blocks of 2900 and 11 800, respectively (Polymer Source, Inc.). The polydispersity index was 1.05. The GPC result showed no sign of the presence of homopolymer in the sample (cf. Supporting Information); the effect of homopolymer on the phase behavior was hence excluded. The volume fraction of PEO (f_{PEO}) in this copolymer was 0.18; therefore, spherical micelles with PEO and PB blocks forming the domain and the corona, respectively, developed through microphase separation in the melt state.

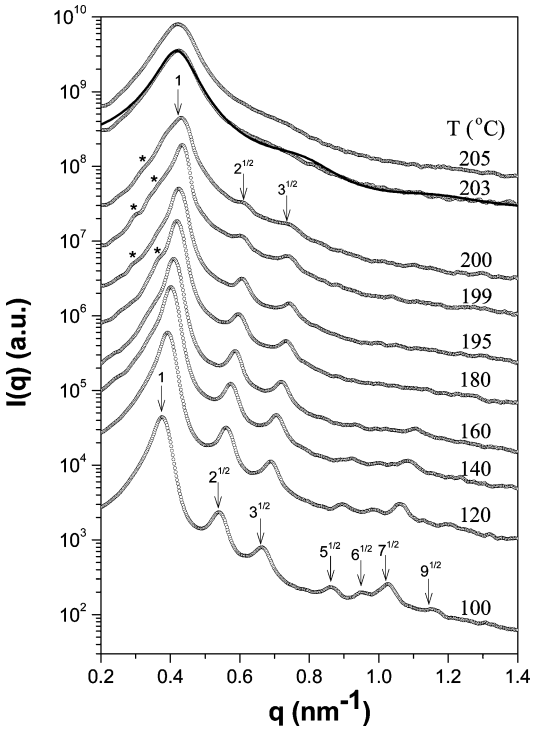

Figure 1. Series of SAXS profiles collected in the heating cycle from the as-cast state to 205 °C. The solid curve in the profile at 203 °C represents the fit by the Percus−Yevick hard-sphere model assuming liquidlike packing of polydisperse spherical domains. The low-*q* satellite peaks marked by an asterisk arise from the large grain structure within the scattering volume.

Temperature-dependent small-angle X-ray scattering (SAXS) experiments were performed under a nitrogen gas atmosphere in a temperature-controlled sample cell. For the measurement at each temperature, the sample was first equilibrated for 30 min, followed by data acquisition for another 30 min. The SAXS apparatus consisted of an 18 KW rotating-anode X-ray generator operated at 30 KV × 400 mA (MAC Science Co, Ltd., Yokohama, now Bruker Co. Ltd., M18XHF, Ibaraki Prefecture, Japan), a graphite crystal for incident beam monochromatization, a 1.5 m camera, and a one-dimensional (1-D) position-sensitive proportional counter with 1024 pixels.

Figure 1 shows the SAXS profiles collected by heating the copolymer from the as-cast state to 205 °C. A series of diffraction peaks with the relative positions of $1:2^{1/2}:3^{1/2}$:...were observed at 100 °C, indicating that the spherical micelles packed in the typical bcc lattice.[11] The bcc phase remained stable up to ca. 200 °C without showing any sign of transformation to the closely packed lattice. It is noted that the "satellite" peaks (marked by an asterisk) appearing beside the primary peak at $T \geq 195$ °C were associated with the relatively large grain structure within the scattering volume for the SAXS experiment using slit collimation and a linear detector with a finite height of window for receiving X-rays.[12] If the 2-D scattering pattern is circularly symmetric, the scattering peaks in the intensity profile are smoothly smoothed. However, when the spotlike

* Corresponding authors. E-mail: hslchen@mx.nthu.edu.tw (H.L.C.); hashimoto.takeji@jaea.go.jp (T.H.).
† Department of Chemical Engineering, National Tsing Hua University.
‡ Advanced Science Research Center, Japan Atomic Energy Agency.

10.1021/ma062149m CCC: $37.00 © 2007 American Chemical Society
Published on Web 01/13/2007

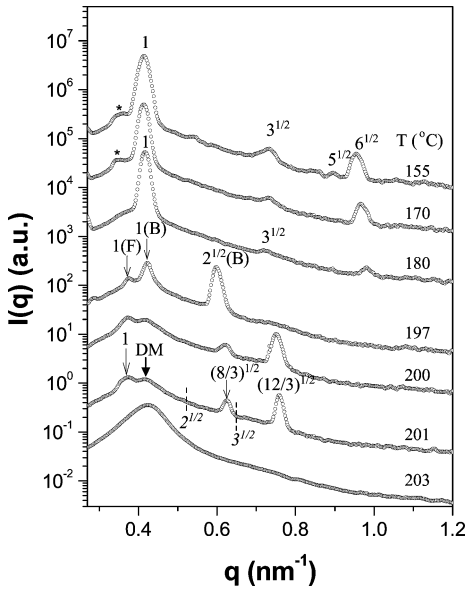

Figure 2. Series of SAXS profiles collected in the cooling cycle. Three fcc peaks with the relative positions 1:$(8/3)^{1/2}$:$(12/3)^{1/2}$ emerge at 201 °C. The vertical dashed lines on the profile at 201 °C mark the positions of the higher-order peaks that would have been exhibited by the bcc lattice.

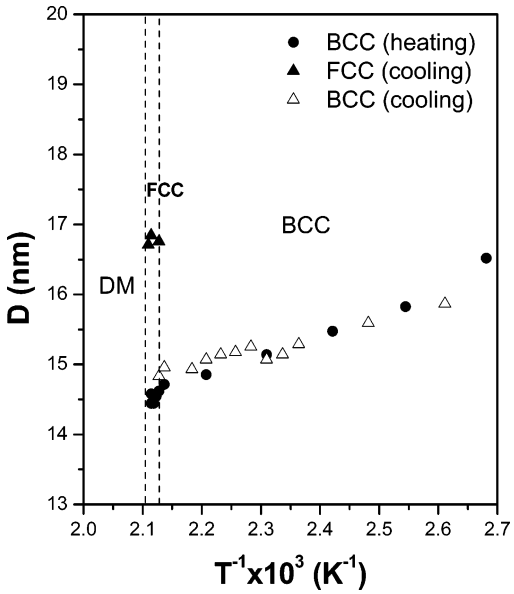

Figure 3. Domain spacing as a function of the inverse of absolute temperature for the heating and the cooling experiments.

scattering patterns from relatively large grains are detected, smeared peaks may appear at q lower than the position of the primary scattering peak (cf. Supporting Information).

The bcc phase transformed into a disordered phase when the temperature was raised to 203 °C, where the corresponding scattering profile showed a broad halo centering at 0.41 nm^{-1} along with a shoulder near 0.7 nm^{-1}. The observed scattering feature was consistent with a disordered micelle (DM) phase[8,9] in which the spherical micelles with liquidlike short-range order interacted through the hard-sphere potential. The solid curve in the scattering profile at 203 °C represents the fit by the Percus−Yevick hard-sphere model, assuming liquidlike packing of polydisperse spherical domains.[13,14] The hard-sphere radius, R_{HS}, considered here, covered an impenetrable shell relevant to the corona surrounding the spherical domain (R_{HS} > radius of PEO sphere, R_c).[14] The parameters obtained from the fit were: the volume fraction of PEO domain $f_c = 0.081$, mean value of $R_c = 4.52$ nm, and $R_{HS} = 7.86$ nm. The significantly smaller f_c in the DM phase than f_{PEO} (= 0.18) indicated that the matrix phase in which the PEO domains were dispersed contained the unconstrained diblocks (i.e., the unimers)[7] and the oligomeric micelles (dimmers, trimers, etc.), which could not be resolved by SAXS. The random thermal motions of these species disturbed the long-range order of the micelles.

Figure 2 shows the temperature-dependent SAXS profiles collected by cooling the copolymer from the DM phase. Three diffraction peaks situated at 0.37, 0.61, and 0.76 nm^{-1} emerged when the system was cooled to 201 °C.[15] The positions of the higher-order peaks relative to that of the primary peak deviated from those (marked by the vertical dashed lines) prescribed by the bcc lattice. Indeed, the peak positions closely followed the ratio of 1:$(8/3)^{1/2}$:$(12/3)^{1/2}$, which were assignable to the (111), (220), and (222) diffraction planes of the fcc lattice, respectively.[11] The fcc phase coexisted with the DM phase, as the broad peak at 0.41 nm^{-1} still persisted and masked the fcc (200) peak locating at $(4/3)^{1/2}$ times the position of the primary peak. The amount of the fcc phase did not increase on further cooling because decreasing the temperature to 200 °C did not essentially alter the scattering profile. As a matter of fact, the scattering pattern remained virtually unaffected by annealing at 200 °C for 5 h, elucidating that fcc was a stable structure coexisting with the DM phase. It is interesting to note that the coexistence of an ordered fcc phase and a disordered phase over a narrow concentration range has also been observed for the crystallization of hard colloids induced by increasing particle concentration.[16]

When the system was further cooled to 197 °C, the originally broad peak at 0.41 nm^{-1} became sharp and intensified. A diffraction peak situating at ca. $2^{1/2}$ times the position of the 0.41 nm^{-1} peak was also visible, showing that a bcc phase had developed upon the cooling. bcc became the predominant packing structure at lower temperatures.[17] The SAXS cooling experiment thus revealed a disorder-to-order transition from DM to fcc phase followed by a DM-to-bcc and a fcc-to-bcc transition. The temperature window of the fcc phase was very narrow (ca. 4 K interval), which was in accord with the prediction by the SCMF calculation.[6] It is noted that the phase behavior of the present system was in clear distinction with that of a sphere-forming blend of a symmetric PEO-*b*-PB with a PB homopolymer in that the blend exhibited a nearly pure fcc phase over a much broader temperature range.[18] This implied that the presence of homopolymer in the matrix phase enhanced the stability of the fcc phase.[19]

Figure 3 plots the domain spacing, D (= $2\pi/q_m$ with q_m being the position of the primary scattering peak), as a function of the inverse of absolute temperature for the heating and the cooling experiments. D was found to decrease abruptly by ca. 11% across the fcc-to-bcc transition on cooling. The domain spacing of bcc and fcc lattices correspond to the spacing of (110) and (111) planes, respectively, given by

$$d_{111}^{\text{fcc}} = \frac{1}{\sqrt{3}}\left(\frac{16\pi}{3f_c}\right)^{1/3} R_c \quad (1)$$

$$d_{110}^{\text{bcc}} = \frac{1}{\sqrt{2}}\left(\frac{8\pi}{3f_c}\right)^{1/3} R_c \quad (2)$$

The larger domain spacing in fcc phase was attributed to the smaller f_c due to the presence of unimers and oligomeric micelles in the matrix phase. The presence of these species had been revealed by the SCMF calculation, which predicted that the domain spacing and the interfacial area underwent an abrupt

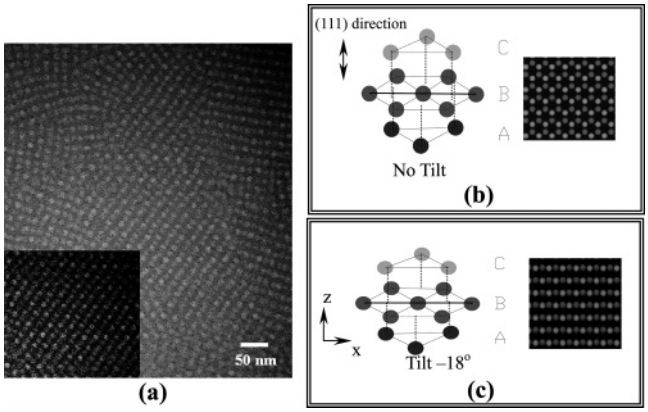

Figure 4. (a) TEM micrograph of PEO-*b*-PB quenched from 200 °C. The (dark) PB phase in the thin section was selectively stained by OsO_4. (b) Schematic illustration showing the generation of fcc lattice by stacking together (111) planes in a ABCABC... sequence (left). The double-layer image on the right corresponds to the projection of fcc lattice onto the plane normal to the (111) direction in a thin section containing B and C layers of spheres, with the spheres in plane B fully contained in the thin section (giving rise to the image of bright spheres) and those in plane C partially contained in the specimen (yielding the image of gray spheres). The image was numerically constructed by assuming the sphere volume fraction of 0.08, which corresponded to that found for the DM phase from which the fcc structure developed. (c) Schematic illustration showing the tilt of the lattice in (b) about the *x*-axis by −18° (left). The resultant TEM image on the right corresponds well to the experimentally observed image in (a), showing regular arrays of spheres with alternating bright and gray contrast along each row or column. This feature can be seen more clearly in the inset of (a), which shows the image with larger contrast.

increase and decrease, respectively, across the OOT from bcc to fcc phase.[7] The reduction of the interfacial area indicated fewer copolymer molecules forming the spherical micelles in the fcc phase as a portion of the minority blocks dissociated from the microdomains, yielding unimers in the matrix phase. As the temperature was lowered, both f_c and R_c increased due to the reduction of unimer concentration and the increase of interfacial tension, respectively. In the transformation from the fcc to the bcc lattice, the effect of the increase of f_c outweighed the increase of R_c, such that d_{110}^{bcc} became smaller than d_{111}^{fcc}, giving rise to a reduction of D observed in Figure 3.

Over the temperature range where the fcc phase coexisted with the DM phase, the primary fcc peak was located at lower q than that associated with the DM phase. It should be noted that, for the DM phase with only short-range order, the Bragg's spacing determined from $2\pi/q_m$ does not have a well-defined physical meaning.[20] The value thus obtained only represents an "apparent" Bragg spacing. In a previous study by Hashimoto et al. on the block copolymer micelles formed in a selective solvent, the apparent Bragg's spacing of the DM phase was found to increase significantly to the real Bragg's spacing of the ordered lattice across the disorder-to-order transition.[20] Such an increase was also predicted by computing the scattering profile associated with the liquid phase within the context of the Born and Green theory on equation of state. Our observation that the primary fcc peak situated at lower q than the scattering peak of the DM phase followed this prediction as the unimers and the oligomeric micelles were considered to behave as the selective solvent for the coronal PB blocks.

The existence of the fcc phase was further verified by transmission electron microscopy (TEM). In this experiment, the sample was cooled from 203 to 200 °C, followed by a rapid quench into liquid nitrogen with the hope that some fcc grains may be preserved for TEM observation. Figure 4a displays the observed TEM micrograph representing only the ordered phase. The micrograph shows an unusual image of regular arrays of spheres with alternating bright and gray contrast along each row or column. We compared the observed image with that derived from a computer graphics program, TEMS, capable of generating the TEM images projected from arbitrary planes in the macrolattices, including bcc and fcc symmetries.[21,22] It is found that the bcc lattice could never generate the image observed in Figure 4a; on the contrary, the fcc lattice could yield the observed image, as shown in Figure 4c. It is known that the fcc lattice can be built by stacking together (111) planes in a ABCABC... sequence, as schematically illustrated in Figure 4b. The TEMS image in Figure 4b shows a double-layer image from the projection of the lattice along the (111) direction in a thin section containing two layers (say, B and C) of spheres, with the spheres in plane B fully contained in the thin section (giving rise to the image of bright spheres) and those in plane C partially contained in the specimen (yielding the image of gray spheres).[18] When this thin section is tilted by about −18° about the *x*-axis [cf. the scheme in Figure 4c], the TEM image transforms into that shown in Figure 4c, which corresponds well to the experimentally observed image. An additional TEM micrograph showing the coexistence of a DM phase, a small fcc grain, and likely a bcc grain in a sample quenched from 197 °C can be found in the Supporting Information.

Now it is worthwhile to consider why fcc would be the favored structure at elevated temperature. The free energy of block copolymer micelles in the melt state mainly consists of two parts, namely the interfacial free energy and the chain conformational free energy. For the micelles packed in an ordered lattice, stretching of the coronal blocks tethered at the domains is not uniform because a portion of them have to stretch more to fit into the vertices of the Wigner-Seitz (W−S) cells to produce a constant-mean-curvature (CMC) surface under the constraint of melt incompressibility.[5] Such a packing frustration increases the conformational free energy and is stronger in the bcc lattice than in the fcc lattice because the corresponding W−S cell in the former is a truncated octahedron, while that in the latter is a rhombic dodecahedron. Therefore, fcc packing is favored in terms of relief of packing frustration. On the other hand, it can be shown that, under given volume fraction of the spherical domain, the surface-to-volume ratio (S/V) of the domains packed in the fcc lattice is 1.03 times that associated with the bcc lattice, i.e., $(S/V)_{fcc} \approx 2^{5/6}(S/V)_{bcc}/3^{1/2} = 1.03(S/V)_{bcc}$, assuming $d_{110}^{bcc} = d_{111}^{fcc}$. At low temperatures where the interblock repulsion is strong, bcc packing is favored, as the reduction of interfacial free energy dominates the cost of conformational entropy loss associated with the packing frustration. Increasing temperature alleviates the effect of interfacial tension; therefore, the spheres split into a smaller size and organize into the fcc lattice once the release of packing frustration outweighs the interfacial free energy contribution.

Although the above argument appears to rationalize the stability of the bcc and fcc phases at low and high temperature, respectively, it is subjected to the speculation that the free energy difference between these two lattices is too small to drive the observed bcc−fcc transition because the nonequilibrium effect such as finite grain size and lattice distortion coupled with thermal fluctuations may easily overwhelm the equilibrium factors discussed above. We hence postulated that the unimers and oligomeric micelles present in the matrix phase, which was not considered above, facilitated the stability of the fcc lattice at elevated temperatures. These species played a similar role to the homopolymer in the blend showing a broader fcc window.

Nevertheless, further studies for resolving their dispersion state in the matrix phase is necessary to elucidate their exact roles.

It is noted that the fcc phase in the present system developed only by cooling from the DM phase, indicating that the bcc-to-fcc transition on heating involved a higher activation energy barrier than the DM-to-fcc transition on cooling. The high activation barrier of the former has also been observed recently by Lodge et al. in a study of the solution of a block copolymer with a selective solvent.[23] Block copolymer micelles have to adjust their internal structure, including the association number and the block chain conformation in response to the temperature change. Increasing temperature decreases the interfacial tension at the domain interface so that the association number of each micelle decreases accordingly to alleviate the stretching of block chains. In this process, a fraction of PEO blocks had to be pulled into the PB matrix, yielding unimers which then diffused through the matrix to assemble to form new micelles. Because the transient mixing between the PEO and PB blocks in the matrix phase was energetically unfavorable due to their strong repulsion, an energetic barrier existed for the pull-out of the PEO blocks. For the present system, the thermal activation energy below 203 °C may not be strong enough to overcome this barrier; consequently, the bcc phase was superheated and directly transformed into the DM phase at sufficiently high temperature. On the other hand, when the system was cooled from the DM phase in which the unimers and oligomeric miclelles were already present, the retrieval of the PEO blocks from the matrix into the existing domains or the assembly of the oligomeric micelles to form larger micelles was relatively easy; therefore, the thermodynamically stable fcc phase could develop spontaneously.

In conclusion, spherical micelles packed in a fcc lattice have been revealed for a neat diblock copolymer in the quiescent melt. This packing symmetry developed upon cooling from a DM phase and coexisted with the DM phase in a narrow temperature region before transforming into bcc structure. We postulated that the fcc phase was stabilized by the unimers and the oligomeric micelles in the matrix phase, as they played a similar role to the homopolymer in the blend exhibiting a broader fcc window.

Acknowledgment. We gratefully acknowledge financial support from the National Science Council Taiwan under contract no. NSC 94 2216-E-007-002.

Supporting Information Available: GPC curve of PEO-*b*-PB, illustration for the origin of the sattelite peaks in the $I(q)$ profile of the sample with relatively large grain structure, TEM micrograph showing the coexistence of DM phase. This material is available free of charge via the Internet at http://pubs.acs.org.

References and Notes

(1) Jones, R. A. L. *Soft Condensed Matter*; Oxford University Press: New York, 2002.
(2) Monovoukas, Y.; Gast, A. P. *J. Colloid Interface Sci.* **1989**, *128*, 533.
(3) Robbins, M. O.; Kremer, K.; Grest, G. S. *J. Chem. Phys.* **1988**, *88*, 3286.
(4) Park, M, J.; Bang, J.; Harada, T.; Char, K.; Lodge, T. P. *Macromolecules* **2004**, *37*, 9064.
(5) Lodge, T. P.; Bang, J.; Park, M. J.; Char, K. *Phys. Rev. Lett.* **2004**, *92*, 145501.
(6) Matsen, M. W.; Bates, F. S. *Macromolecules* **1996**, *29*, 1091.
(7) Matsen, M. W.; Bates, F. S. *J. Chem. Phys.* **1997**, *106*, 2436.
(8) Sakamoto, N.; Hashimoto, T.; Han, C. D.; Kim, D.; Vaidya, N. Y. *Macromolecules* **1997**, *30*, 1621.
(9) Sakamoto, N.; Hashimoto, T. *Macromolecules* **1998**, *31*, 8493.
(10) Dormidontova, E. E.; Lodge, T. P. *Macromolecules* **2001**, *34*, 9143.
(11) Cullity, B. D.; Stock, S. R. *Elements of X-Ray Diffraction*; Prentice Hall: Upper Saddle River, NJ, 2001; Chapter 10.
(12) Kimishima, K.; Koga, T.; Hashimoto, T. *Macromolecules* **2000**, *33*, 968.
(13) Percus, J. K.; Yevick, G. J. *Phys. Rev.* **1958**, *110*, 1.
(14) Kinning, D. J.; Thomas, E. L. *Macromolecules* **1984**, *17*, 1712.
(15) The assertion that the three scattering peaks observed at the relative peak positions of $1:(8/3)^{1/2}:(12/3)^{1/2}$ were associated with the fcc lattice might be subjected to suspicion that the peak located at 0.37 nm^{-1} was the satellite peak of the primary peak that was masked by the DM peak at 0.41 nm^{-1}; in that case, the actual diffraction peaks were located at 0.41, 0.61, and 0.76 nm^{-1}. However, we did not consider the peak at 0.37 nm^{-1} to be the satellite peak because this peak was reproducible in terms of its intensity and position relative to those of the DM peak for the experiments using three independent samples. Such a reproducibility was not expected for a satellite peak because the intensity and position of the satellite peak depended on the orientation of the large grains with respect to the incident beam and such an orientation varied from one sample to another. Moreover, if the actual diffraction peaks were located at 0.41, 0.61, and 0.76 nm^{-1}, then their relative position of 1:1.49:1.85 deviated from that prescribed by the bcc lattice (i.e., 1:1.41:1.73). Consequently, the actual diffraction peaks were identified as those at 0.37, 0.61, and 0.76 nm^{-1}. In this case, the position ratio was 1:1.65:2.05, which closely agreed with that (1:1.63:2.0) prescribed by the fcc lattice.
(16) Russel, W. B.; Saville, D. A.; Schowalter, W. R. *Colloidal Dispersions*; Cambridge University Press: New York, 1989; Chapter 10.
(17) The first three bcc scattering peaks exhibit the relative position of $1:2^{1/2}:3^{1/2}$. The $2^{1/2}$ peak showed up clearly in the profile collected at 197 °C in Figure 2, while the $3^{1/2}$ peak was hardly discernible. By contrast, the $2^{1/2}$ peak was absent in the profiles collected at 180, 170, and 155 °C, whereas the $3^{1/2}$ peak was visible. Both $2^{1/2}$ and $3^{1/2}$ peaks were visible in the scattering profiles collected by heating in Figure 1. The diminishment of the scattering peaks was again attributable to the relatively large grains developed during cooling from the DM phase, as illustrated in the Supporting Information. Because the grains were able to rotate when the temperature of the specimen was changed during the SAXS measurement, their orientations with respect to the incident beam may vary from one temperature to another, thereby leading to 2-D patterns with different distributions of the scattering spots at different temperatures. For the heating experiment leading to the SAXS profiles in Figure 1, the sample contained small grains such that the 2-D scattering patterns at various temperatures were circularly symmetric; as a result, both $2^{1/2}$ and $3^{1/2}$ peaks were observable. For the sample containing a small number of relatively large grains that give rise to a series of diffraction spots, the relative intensities of the scattering peaks collected by the linear detector should be carefully treated for further analysis because the intensities along the linear detector strongly depend on the grain orientations, which change with temperature in the cooling experiment due to grain rotations. However, the relative positions of the peaks appeared in the 1-D intensity profile are still reliable for identifying the type of lattice structure if a sufficient number of peaks are present.
(18) Huang, Y.-Y.; Chen, H.-L.; Hashimoto, T. *Macromolecules* **2003**, *36*, 764.
(19) Matsen, M. W. *Macromolecules* **1995**, *28*, 5765.
(20) Hashimoto, T.; Shibayama, M.; Kawai, H.; Watanabe, H.; Kotaka, T. *Macromolecules* **1983**, *16*, 361.
(21) Nishikawa, Y.; Kawada, H.; Hasegawa, H.; Hashimoto, T. *Acta Polym.* **1993**, *44*, 247.
(22) Nishikawa, Y. Interfacial Curvatures of Bicontinuous Phase Structures in Two-Component Polymeric Systems. Ph.D. Thesis, Kyoto University, 1999.
(23) Bang, J.; Lodge, T. P. *Phys. Rev. Lett.* **2004**, *93*, 245701.

MA062149M